Disruption of a *Plasmodium falciparum* gene linked to male sexual development causes early arrest in gametocytogenesis

Tetsuya Furuya*, Jianbing Mu*, Karen Hayton*, Anna Liu*, Junhui Duan*, Louis Nkrumah†, Deirdre A. Joy*, David A. Fidock†, Hisashi Fujioka‡, Akhil B. Vaidya§, Thomas E. Wellems*, and Xin-zhuan Su*¶

*Laboratory of Malaria and Vector Research, National Institute of Allergy and Infectious Diseases, National Institutes of Health, Bethesda, MD 20892-8132; †Department of Microbiology and Immunology, Albert Einstein College of Medicine, Bronx, NY 10461; ‡Institute of Pathology, Case Western Reserve University, Cleveland, OH 44106; and §Department of Microbiology and Immunology, Drexel University College of Medicine, Philadelphia, PA 19129

Edited by Louis H. Miller, National Institutes of Health, Rockville, MD, and approved September 27, 2005 (received for review March 8, 2005)

A male gametocyte defect in the *Plasmodium falciparum* Dd2 parasite was previously discovered through the observation that all progeny clones in a Dd2 × HB3 genetic cross were the result of fertilization events between Dd2 female and HB3 male gametes. A determinant linked to the defect in Dd2 was subsequently mapped to an 800-kb segment on chromosome 12. Here, we report further mapping of the determinant to an 82-kb region and the identification of a candidate gene, *P. falciparum* male development gene 1 (*pfmdv-1*), that is expressed at a lower level in Dd2 compared with the wild-type normal male gametocyte-producing ancestor W2. Pfmdv-1 protein is sexual-stage specific and is located on the gametocyte plasma membrane, parasitophorous vacuole membrane, and the membranes of cleft-like structures within the erythrocyte. Disruption of *pfmdv-1* results in a dramatic reduction in mature gametocytes, especially functional male gametocytes, with the majority of sexually committed parasites developmentally arrested at stage I. The *pfmdv-1*-knockout parasites show disturbed membrane structures, particularly multimembrane vesicles/tubes that likely derive from deformed cleft-like structures. Mosquito infectivity of the knockout parasites was also greatly reduced but not completely lost. The results suggest that *pfmdv-1* plays a key role in gametocyte membrane formation and integrity.

gametocyte | genetic mapping | malaria | microarray

The life cycle of the malaria parasite *Plasmodium falciparum* includes sexual reproductive events as well as multiple rounds of asexual replication in the mosquito and human hosts. Although diploid for a short time after zygote formation in the mosquito (1, 2), the malaria parasite carries a haploid genome for most of its life cycle. There are no known sex chromosomes in the parasite genome, and parasite lines derived from a single individual cell (clone) are capable of producing both male and female gametocytes. A malaria parasite therefore has three choices after a round of asexual reproduction: (*i*) continue the asexual reproduction cycle, (*ii*) develop into a male gametocyte, or (*iii*) develop into a female gametocyte. The switch from the asexual to sexual stages is most likely regulated by signal transduction and gene expression. Examples of agents that have been reported to trigger the switch to sexual development include parasite lysates, conditioned medium, antimalarial drugs, antibodies, temperature changes, pH variation, and chemicals such as cAMP and berenil (3–16). Most of the effects, however, have been difficult to reproduce because of a high degree of experimental variability (15). When merozoites released from a single sexually committed schizont become gametocytes, they are either all males or all females, suggesting that the commitment to differentiate into male or female is likely to occur before the nuclear division of the sexually committed schizont (17–19); however, the precise stage of parasite commitment or the signals involved in sexual differentiation are unknown.

The ability to produce gametocytes is often diminished or completely lost after extended *in vitro* culture. One example is the Dd2 clone, which has greatly reduced capability to produce male gametocytes relative to normal production by other parasite lines such as HB3 and W2 (20, 21). This defect arose after a series of experimental manipulations, including *in vitro* drug pressure and cloning from Dd2's ancestor W2 (22, 23). Because the Dd2 parasite was one of the parents of the Dd2 × HB3 genetic cross (24), it proved possible to link a determinant of male gametocyte development phenotype in Dd2 to an 800-kb segment of chromosome (chr)12 (20, 25). Here, we further localize the defect determinant to an 82-kb segment on chr12 and identify a candidate gene, *P. falciparum* male development gene 1 (*pfmdv-1*), that plays an important role in gametocyte development.

Methods

Parasite Culture, Gametocyte Production, and Exflagellation Determinations. *P. falciparum* was cultured as described (26). For gametocyte cultures, sorbitol-synchronized trophozoites diluted to 0.2–0.5% parasitemia were cultured with daily medium changes until mature gametocytes were obtained. Exflagellation was triggered by adding 20 μl of human type O^+ serum to day 14–16 gametocytes pelleted from 1 ml of culture, and mobile exflagellation centers were counted under a microscope. A ratio of the exflagellation center counts to gametocytemia (REC) was obtained by dividing the exflagellation center counts per 60 fields by the mean gametocytemia (percentage of erythrocytes containing gametocytes in three separate culture flasks) to adjust for variation in gametocytemia among different cultures.

DNA Sequencing and Genetic Mapping. Quantitative trait loci linked to the male gametocyte defect in Dd2 were analyzed by using methods described in ref. 27. The genotypes of the progeny used in this study were determined as previously described in ref. 28. The coding regions of the 29 predicted genes from both Dd2 and W2 in the *mdv* locus were amplified and sequenced by using methods previously described in ref. 29. Nucleotide substitutions and size polymorphisms were identified from the aligned sequences.

Microarray Analysis and Real-Time RT-PCR. RNAs were isolated by using TRIzol reagent (Invitrogen) from saponin-treated parasite pellets. cDNA samples from total RNAs primed with both $(dT)_{12–20}$

MICROBIOLOGY

Conflict of interest statement: No conflicts declared.

This paper was submitted directly (Track II) to the PNAS office.

Freely available online through the PNAS open access option.

Abbreviations: chr, chromosome; CLS, cleft-like structure; KO, knockout; MMS, multimembrane structure; MS, microsatellite; OB, osmiophilic bodies; PM, plasma membrane; PVM, parasitophorous vacuolar membrane; REC, ratio of exflagellation center counts to gametocytemia.

¶To whom correspondence should be addressed at: Laboratory of Malaria and Vector Research, Room 3E-24B, 12735 Twinbrook Parkway, Rockville, MD 20850. E-mail: xsu@niaid.nih.gov.

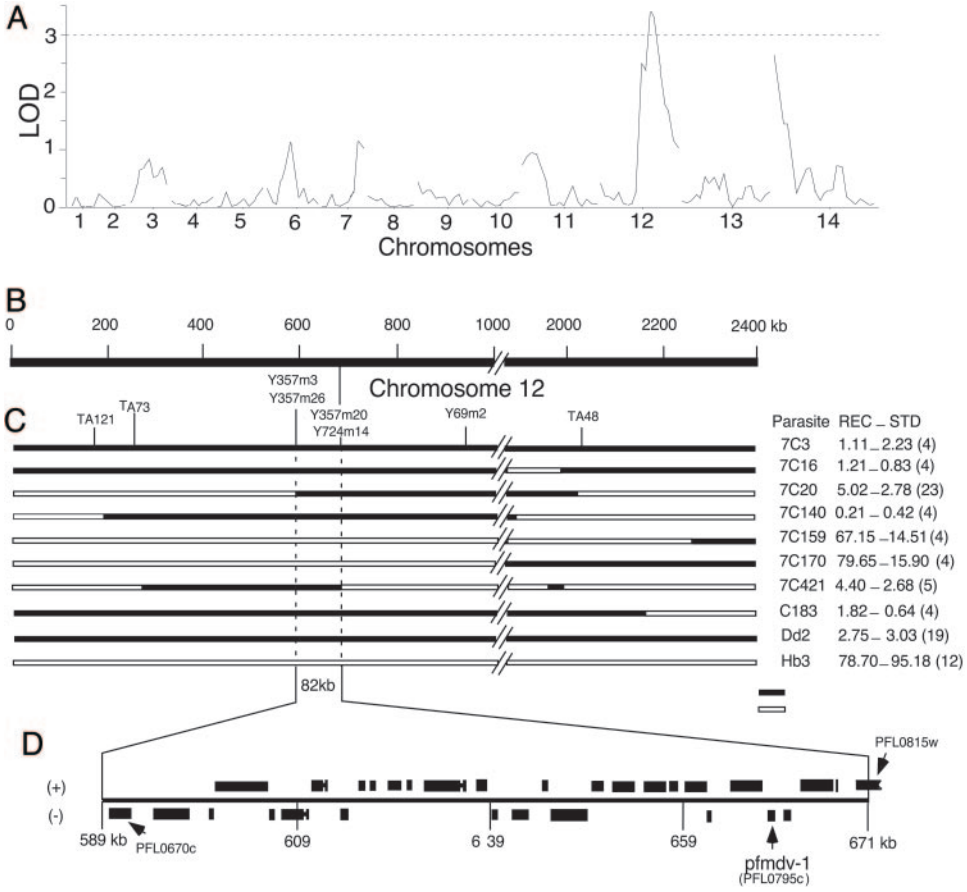

Fig. 1. Mapping of a determinant underlying the male gametocyte development defect in the Dd2 parasite. (*A*) Genome-wide scan for loci linked to a defect in male gametocyte development by using progeny from the Dd2 × HB3 cross and MSs from a linkage map (28). A major peak with a lod (logarithm of odds) score of ≈3.5 on chr12 and a secondary peak of ≈2.5 on chr14 were identified by using methods described in ref. 27. (*B*) A physical map of chr12 showing a 2,400-kb segment containing the *mdv* locus. (*C*) Genotypes (solid dark lines, Dd2 type; open lines, HB3 type) and phenotypes of eight selected progeny having either the parental genotype or crossovers on chr12. REC (±SD) is the ratio of the mean number of exflagellation centers to the mean gametocytemia of day 14–16 cultures. Progeny 7C159 and 7C170 have a phenotype (REC) similar to that of HB3, whereas the phenotypes of other progeny are similar to that of Dd2. The values in parentheses indicate the number of experiments repeated in independent culture flasks. Positions of selected MS markers are indicated above the genotype lines. MSs Y357m26 and Y724m14 lie outside two informative crossovers in progeny 7C20 and 7C421 that define an 82-kb region containing the *mdv* determinant. (*D*) Twenty-nine predicted genes in the *mdv* locus. The candidate gene is marked as *pfmdv-1*. Detailed annotation of the genes can be found at PLASMODB.

primer and random hexamers were labeled with dUTP-Cy3 or dUTP-Cy5 according to the manufacturer's instructions (Amersham Pharmacia Biosciences) and hybridized to microarray slides printed with 7,462 70-mer oligonucleotides (Qiagen, Valencia, CA) (30). For detailed microarray hybridizations and real-time RT-PCR procedures, see *Supporting Text*, which is published as supporting information on the PNAS web site.

Generation of *pfmdv-1*-Knockout (KO) Parasite Lines. *pfmdv-1*-disrupted lines were generated by using a negative selection system (31). Two DNA fragments, each including 5′ or 3′ portions of the *pfmdv-1* ORF and flanking noncoding regions [PLASMODB (www.plasmodb.org) chr12 nucleotides 658542–657686 for 5′ and 657598–656662 for 3′ portions] were amplified from W2 genomic DNA and inserted into two of the multiple cloning sites flanking the human dihydrofolate reductase (hDHFR) cassette (Fig. 6*A*, which is published as supporting information on the PNAS web site). The W2 parasite was mixed with erythrocytes previously electroporated with the plasmid constructs (50 μg) with or without the *pfmdv-1* sequence according to the procedures described in ref. 32. WR99210 was added to a final concentration of 5 nM 2 days after infection to select for parasites carrying the construct. After parasites were established in culture 4 weeks after addition of WR99210, ganciclovir was added to a 4 μM final concentration for 9 days. After growing in drug-free medium for 14 days, the parasites were again grown under 5 nM WR99210. The selected parasites were cloned by using limiting dilution in 96-well plates at 0.25–2 cells per well. Integration of the insert into the chromosome and disruption of the *pfmdv-1* gene were first detected by using an allelic-specific PCR and confirmed by Southern blotting.

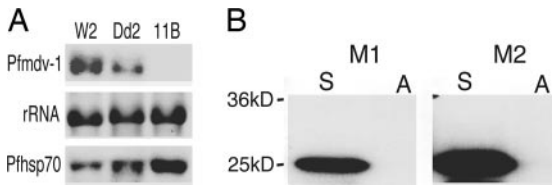

Fig. 2. Expression of *pfmdv-1* in sexual stages. (*A*) Northern blot hybridization showing lower-level transcription of *pfmdv-1* in day 6 Dd2 sexual stages and absence of *pfmdv-1* transcript in the *pfmdv-1*-KO parasite 11B. Transcripts from *pfhsp70* and rRNA were used to verify equivalent sample loading in each lane. (*B*) Immunoblot showing an ≈25-kDa protein band recognized by mouse antisera against a peptide at the C terminus (CKTKNPDLDEQTKDIKTHSDS) of Pfmdv-1. M1 and M2 are sera from two individual mice; S and A represent lysates from sexual and asexual stages, respectively.

Mosquito Infection. Mature gametocytes were fed to *Anopheles stephensi* mosquitoes by using a membrane-feeding apparatus as described in ref. 33. Before mosquito feeding, the gametocytemia from different parasite lines was adjusted to the same percentage (0.01% or 0.1%) at 40% hematocrit. Mosquito midguts were dissected 9 days after feeding and were stained with 0.1% Mercurochrome and counted by light microscopy.

Other Methods. Procedures for microarray hybridization and analysis, Southern blotting, Northern blotting, protein blotting, antibody production, indirect immunofluorescence assay, immunoelectron microscopy, and transmission electron microscopy can be found in *Supplemental Materials*.

Results

Mapping the *pfmdv-1* Gene to an 82-kb Segment on chr12. To locate the gene(s) responsible for the male gametocyte development

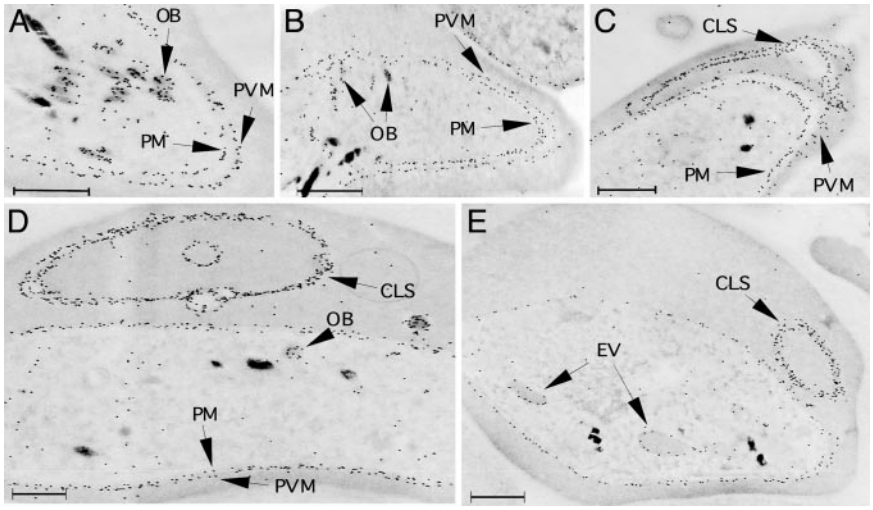

Fig. 3. Immunoelectron microscopy localization of Pfmdv-1 in developing W2 gametocytes. (*A*) A partial gametocyte image showing Pfmdv-1 at the PM, PVM, and in secretory OB. (*B*) A gametocyte with Pfmdv-1 in OB potentially merging with parasite PM. (*C*) A gametocyte with PVM extending into a CLS. Note the continuation of PVM into the CLS. (*D*) Cross section of a large CLS and its extension branches (small circles) from a late-stage gametocyte. (*E*) A young gametocyte with two engulfing vesicles (EV) having materials similar to erythrocyte cytoplasm surrounded by a single membrane containing Pfmdv-1. (Scale bars: 1 μm.)

defect in the Dd2 parasite, we used a set of 28 progeny from the Dd2 × HB3 cross and a corresponding high-density microsatellite (MS) map (28) to map meiotic crossovers inside the 800-kb segment previously shown to harbor *pfmdv-1* (25) (Fig. 1). Gametocyte production and exflagellation phenotypes from 19 progeny, including 2 of the 11 progeny typed in a previous report (20), were analyzed for loci contributing to the phenotype. To adjust for laboratory variations in gametocytemia between experiments, we used REC as a measure of phenotype. The HB3 parent typically showed a REC of 50 or higher, whereas the Dd2 parent showed a REC < 10. Analysis of the REC and genotypes from the progeny suggested that, in addition to a major determinant on chr12 locus, a secondary determinant on chr14 might also contribute to the phenotype (Fig. 1*A*). A close examination of progeny with crossovers at the 800-kb locus suggested that the determinant affecting the male gamete defect phenotype was located within an ≈82-kb DNA segment of chr12 (Fig. 1*C*). Progeny 7C159 and 7C170 have average REC of 67 and 80, respectively, indicating an HB3-like phenotype, whereas the remaining six progeny showed an average REC of < 6, corresponding to the Dd2-like phenotype. Comparison of MS inheritance and progeny phenotypes allowed us to refine the locus to a chromosome segment one-tenth of that previously mapped. A crossover marked by MS markers Y357m26 and Y357m3 in progeny 7C20 at one end and another crossover marked by MS markers Y724M14 and Y357M20 in progeny 7C421 at the other end located the determinant within an 82-kb DNA segment containing 29 predicted genes as annotated in PLASMODB (gene ID from PFL0670c to PFL0815w) (Fig. 1*D*).

Sequence Comparison of Predicted Genes in the 82-kb Locus. We sequenced the coding regions of the 29 predicted genes in the 82-kb locus from the isogenic parasite pair W2 and Dd2 to search for polymorphisms potentially responsible for the phenotype change (Table 2, which is published as supporting information on the PNAS web site). Dd2 was derived from W2, a clone that produces normal numbers of male gametocytes (20, 21). No sequence differences in the coding sequences of the 29 predicted genes were found between the W2 and Dd2 parasites, although many nucleotide substitutions and MS polymorphisms were present between 3D7 and W2/Dd2. The defect, however, may not be caused by changes in coding regions and can be due to changes or chromatin modification in noncoding regulatory regions that may affect gene expression. Next, we considered whether the male gametocyte-development defect might be attributed to changes in gene expression not involving coding changes in the 82-kb segment.

***pfmdv-1* Is Down-Regulated in Sexual Stages of the Dd2 Parasite.** To search for gene expression differences between the Dd2 and W2 parasites, we compared the transcription profiles of 4,488 annotated and 1,315 unannotated *P. falciparum* ORFs, including all of the 29 genes in the 82-kb locus on chr12, on microarrays printed with 7,462 70-mer oligonucleotides (30) (Qiagen, Valencia, CA). Signals from 12 predicted ORFs were markedly down-regulated, and 27 others were up-regulated in Dd2 relative to W2 at day 8 (Table 3, which is published as supporting information on the PNAS web site). One of the down-regulated genes in Dd2 (PFL0795c) was localized to the 82-kb chr12 segment and is expressed only in sexual stages according to proteomic and microarray data (30, 34–36). Therefore, we term the gene *pfmdv-1*, *P. falciparum* male gametocyte development gene 1, as a candidate gene for the defect locus. Down-regulation of *pfmdv-1* in Dd2 relative to W2 was confirmed by using real-time RT-PCR (Table 3) and RNA blotting (Fig. 2*A*).

***pfmdv-1* Encodes an ≈25-kDa Protein Expressed in Gametocyte Stages I–V.** The gene annotation programs PHAT and GLIMMERM predict that *pfmdv-1* has a single exon and encodes a protein of 221 aa (PLASMODB database). Further searches of PLASMODB identified multiple expressed sequence tags that span *pfmdv-1*, including the 663-bp ORF predicted by PHAT and GLIMMERM, a 332-bp 5′ and a 56-bp 3′ untranslated regions.

Analysis of the amino acid sequence showed that the protein contains a predicted signal peptide/transmembrane domain that is conserved in some orthologs of primate and rodent parasites (Fig. 7, which is published as supporting information on the PNAS web site). Comparative alignments of Pfmdv-1 and its homologs showed aa identity ranging from 39% (*Plasmodium yoelii*) to 94% (*Plasmodium reichenowi*), with well conserved domains in the center of the predicted protein (Fig. 7). No molecules with significant homology to Pfmdv-1 were found in the databases of other organisms.

To study the expression of Pfmdv-1, we generated mouse polyclonal antibodies against the protein by using three keyhole limpet hemocyanin-conjugated peptides from the predicted amino acid sequence (amino acids 31–50, CIGKPQVNTNGKNVNSNEKAN; amino acids 173–192, CVPFEENNKSGNANEETENFV; and

MICROBIOLOGY

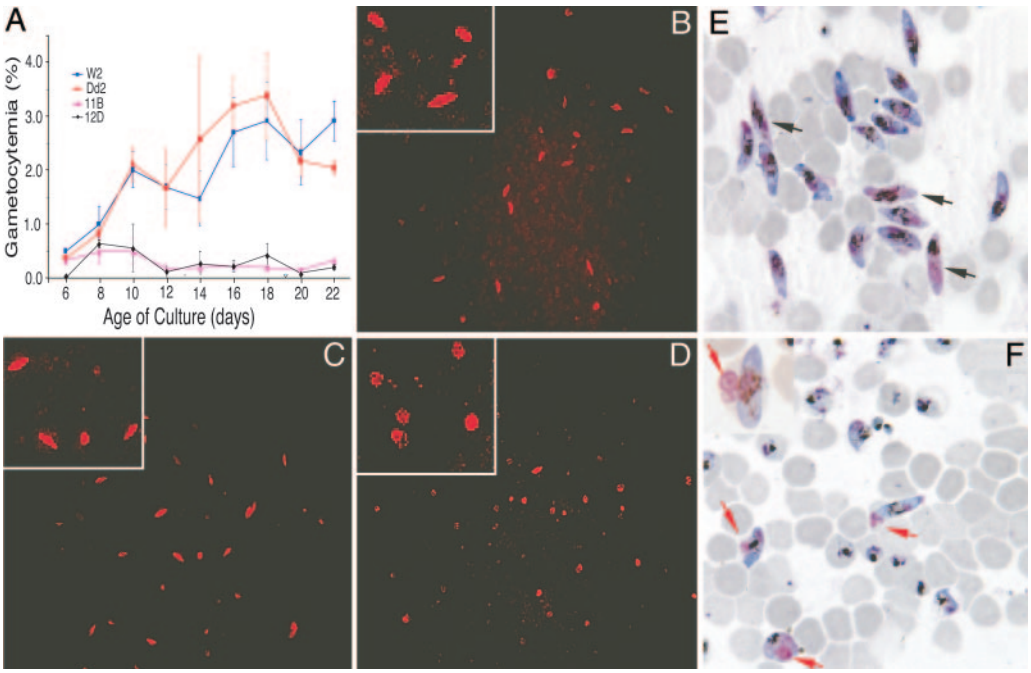

Fig. 4. Reduced gametocytemia and arrested gametocyte development in *pfmdv-1*-KO lines. (*A*) Plots of gametocytemia show dramatic reduction in the numbers of elongated stage III–V gametocytes in *pfmdv-1*-KO lines 11B and 12D compared with W2 and Dd2. Standard errors are from three independent cultures that were initiated simultaneously. (*B–D*) Day-14 sexual stages from W2 (*B*), Dd2 (*C*), and 11B (*D*) were stained with mouse monoclonal anti-Pfg27 antibody and goat anti-mouse Texas-red-conjugated secondary antibodies. Pfg27 is a sexual-specific protein that is expressed in early gametocytes. Note that the majority of stained cells in 11B are an abnormally round shape, whereas those in W2 are elongated stage IV–V. Dd2 shows many abnormal forms among normal-appearing elongated gametocytes. (*E* and *F*) *N*-acetylglucosamine-treated and Percoll–sorbitol-purified day-15 gametocytes from W2 (*E*) and 11B (*F*) were Giemsa-stained and examined by microscopy. Black arrows indicate W2 male gametocytes with pink cytoplasm (*E*), and red arrows point to a residual body present in some 11B gametocytes (*F*). *Insets* in *B–D* and *F* show enlarged parasite images.

amino acids 201–220, CKTKNPDLDEQTKDIKTHSDS) (Fig. 7). Mouse antibodies against peptide sequence (amino acids 201–220) specifically detected an ≈25-kDa protein in lysates of gametocytes but not in asexual parasite stages (Fig. 2*B*), in agreement with the single-exon prediction of a 25.6-kDa protein expressed in sexual stages only. These results are also consistent with Pfmdv-1 enzymatic fragments present in the proteome databases of gametocyte and gamete lysates (34, 35).

We also investigated the cellular localization and expression of Pfmdv-1 by immunofluorescence assay on parasites of different sexual developmental stages. Pfmdv-1 was detected by immunofluorescence assay in all erythrocytic sexual stages, peaking at stage III–IV gametocytes and gradually diminishing in stage V mature gametocytes (Fig. 8, which is published as supporting information on the PNAS web site). Microscopic images from immunofluorescence assays showed a diffuse expression pattern, possibly cytoplasmic, in stage I and II gametocytes, strong staining associated with the membrane of stage III–IV gametocytes (Fig. 8*A*), and localization to an unknown structure in the center of the mature gametocytes (Fig. 8*B*). Signal quantification from confocal microscopic images, taken under the same conditions, confirmed that Pfmdv-1 expression is indeed decreased in Dd2 relative to W2 parasites, consistent with the microarray and real-time RT-PCR results (Fig. 8*C*). In contrast, *pfmdv-1*-KO parasites were not stained by either mouse or rabbit anti-Pfmdv-1 antibodies, suggesting that the antibodies are specific to Pfmdv-1 protein (Fig. 8*D*).

Immunoelectron microscopy revealed localization of Pfmdv-1 on the gametocyte plasma membrane (PM), parasitophorous membrane (PVM), and cleft-like structures (CLSs) that appear as striking extensions of PVM (Fig. 3). Pfmdv-1 was also detected in specific secretory vesicles, termed osmiophilic bodies (OB), within gametocytes (Fig. 3 *A*, *B*, and *D*). These may be involved in transporting Pfmdv-1 to the parasite PM and PVM. After transport to the parasite PM, Pfmdv-1 may reenter the parasite cytoplasm by vesicles that engulf erythrocyte cytoplasm (Fig. 3*E*).

Disruption of *pfmdv-1* Produces Developmental Arrest of Early Sexual Stages. To study its role in gametocyte development, we disrupted the *pfmdv-1* gene in the W2 parasite clone by using the WR99210 positive selection and thymidine kinase negative selection system (31) and evaluated the effect of the resulting KO on gametocyte development (Fig. 6*A*). The presence of *pfmdv-1* KO parasites in the transfected cultures was detected by PCR after negative selection (Fig. 6*B*) and confirmed by Southern (Fig. 6*C*) and Western (Fig. 6*D*) blotting. Parasites with disrupted *pfmdv-1* were cloned by using limiting dilution, and two clones (11B and 12D) were selected for further assessment.

Disruption of the *pfmdv-1* gene did not affect the growth or survival of asexual erythrocyte-stage parasites, consistent with observations that *pfmdv-1* is expressed only in sexual stages; however, obvious effects were observed in the sexual gametocyte stages. Markedly fewer stage III–V gametocytes were obtained from the KO clones than from the W2 parasite (3–6% of W2) (Fig. 4*A*). The majority of sexually committed parasites from the KO lines remained arrested at stage I, while those from W2 continued to develop normally, resulting in a gradual increase in the number of maturing gametocytes (Fig. 4 *B–D*). Although very few elongated gametocytes were present in late cultures (day 14 or later), many stage I-like gametocytes could still be seen in the KO lines (Fig. 4*D*). We also examined pure gametocyte populations separated by Percoll-Sorbitol fractionation after *N*-acetylglucosamine treatment to kill asexual stages. Giemsa staining of enriched W2 parasites showed abundant healthy female and male gametocytes (distinguished by blue and pink cytoplasm after Giemsa staining, respectively; Fig. 4*E*), whereas few developed gametocytes were observed in the 11D KO population (Fig. 4*F*). Additionally, the majority of

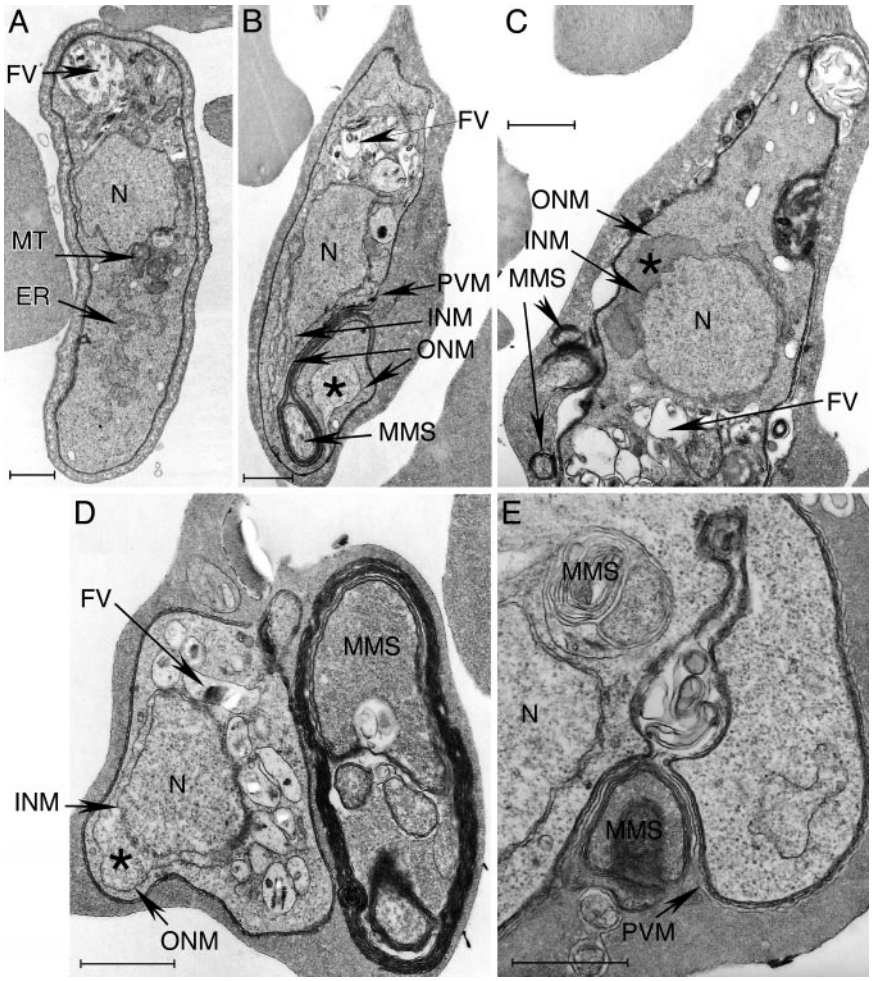

Fig. 5. Transmission electron microscopy of W2 and 11B KO gametocytes. (*A*) A normal gametocyte from W2 parasite showing nucleus (N), endoplasmic reticulum (ER), food vacuole (FV), and mitochondria (MT). (*B–E*) Various sexual stages from *pfmdv-1*-disrupted parasite 11B. (*B*) An elongated gametocyte with an enlarged nucleus and separated inner nuclear membrane (INM) and outer nuclear membrane (ONM) with moderately dense materials accumulated within the space (*). A developing MMS is also present. A multimembrane forms a spiral-like configuration that appears to be a direct extension of the PVM. (*C*) An elongated gametocyte with a dislocated ONM and some small MMS within the parasitophorous space and erythrocyte cytoplasm. (*D*) A ''young'' gametocyte with a large MMS in erythrocyte cytoplasm. Again, moderately dense materials in the perinuclear space (*) can be seen. (*E*) Developing and secreting MMS. A membrane-bound MMS near the nucleus and an MMS developing inside the parasitophorous space and/or closely associated with the PVM are shown. (Scale bars: 1 μm.)

the elongated gametocytes from 11B KO parasites showed a pink-stained structure (red arrow) that was peripheral to the main body of the cells and was not observed in healthy W2 gametocytes (Fig. 4*F*). We also counted male and female gametocytes on the slides shown in Fig. 4 *E* and *F*. To our best judgment, male/female ratio for W2 is 0.145 (29/200) and 0.025 for 11B (5/200, counting elongated mature-looking parasites only), although we recognize that these counts may be subjective. These ratios are similar to those reported for W2 and Dd2 (21).

***pfmdv-1*-Null Parasites Develop Abnormal Membrane Structures in Erythrocyte Cytoplasm.** Under transmission electron microscopy, various changes were observed in the *pfmdv-1*-disrupted parasites when compared with healthy W2 gametocytes (Fig. 5*A*): (*i*) enlargement of the nucleus and/or accumulation of materials in the perinuclear space between the inner and outer nuclear membranes (Fig. 5 *B–D*); (*ii*) formation of multimembrane structures (MMS), either vesicles or CLSs extending from the parasitophorous space into erythrocyte cytoplasm (Fig. 5 *B–E*) that likely correspond to the pink staining seen in Giemsa-stained parasites (Fig. 4*F*) as well as similar structures seen in the immunoelectron microscopy pictures (Fig. 3 *C–E*); and (*iii*) the presence of single membrane vacuoles with moderately dense material near the nucleus (Fig. 5 *B–D*). These changes and membrane localization suggest that Pfmdv-1 plays an important role in maintaining membrane structures essential to gametocyte maturation in erythrocytes.

Dd2 and *pfdmv-1*-KO Parasites Produce Fewer Functional Male Gametocytes than W2. Very few exflagellation centers were observed in the KO lines, whereas a substantial number of exflagellating

Table 1. Exflagellation center counts and mosquito infectivity from day-14 gametocyte cultures

	Exflagellation			Mosquito infectivity		
Parasite	Mean exflagellation centers* (±SE)	Mean gametocytemia, % (±SE)	REC	% Infected	Mean oocyst count†	Infectivity index
W2	1.50 ± 0.47	1.74 ± 0.29	61.2	58	1.35	78.2
Dd2	0.13 ± 0.05	2.57 ± 0.89	3.0	17.5	0.41	5.8
11B	0.01 ± 0.01	0.20 ± 0.01	3.3	10	0.13	2.5
12D	0.01 ± 0.01	0.27 ± 0.13	2.4	15	0.20	6.0

*Mean exflagellation center counts per field calculated from three separate cultures.
†Averaged from two independent feeds.

MICROBIOLOGY

gametes were observed in W2 gametocyte cultures (Table 1). Additionally, the *pfmdv-1* KO appeared to affect male gametocyte development more than female gametocyte development, because the REC indices of the KO parasites were also markedly reduced, similar to those seen in Dd2 (Table 1).

***pfmdv-1* KO Parasites Are Poorly Infective to Mosquitoes.** Equal numbers of day-15 gametocytes from W2, Dd2, and the *pfmdv-1*-KO lines 11B and 12D were fed to *A. stephensi* mosquitoes. Nine days after feeding, the mosquito midguts were dissected and examined under the microscope for the presence of oocysts. Mosquitoes fed with 11B, 12D, and Dd2 gametocytes harbored significantly fewer oocysts than those fed with W2 (χ^2 test, $P < 0.005$ for all tests) (Table 1). The infectivity index was also markedly reduced in Dd2 and the KO parasites. These results show that, although the *pfmdv-1*-KO lines can still produce small numbers of mature, competent gametocytes for fertilization, the absence of Pfmdv-1 greatly compromises the ability of these gametocytes to infect mosquitoes.

Discussion

The male gametocyte-defect phenotype was initially discovered through the observation that all progeny clones in the Dd2 × HB3 genetic cross were derived from Dd2 female and HB3 male gametes (37). Further examination of gametocyte development revealed that Dd2 had a substantially impaired ability to produce competent male gametes, providing an explanation for the predominant maternal organelle inheritance from Dd2 in the genetic cross. The defect, however, does not completely block parasite sexual development, because gametocytes from the Dd2 parasite still produce some fertilization-competent male gametes, resulting in oocysts in mosquito midguts that were fed with Dd2 alone. The defect has been quantified by using a mosquito infectivity index (the product of the mean oocyst count per gut and the percentage of mosquitoes containing one or more oocysts) and exflagellation center counts (20). Employing these quantitative measurements, we have found that *pfmdv-1*-KO lines produce even fewer gametocytes than Dd2 (<10%), with evidence that female gametocytes are affected along with more dramatic effects on males.

In Dd2, the majority of the sexual stages develop into elongated gametocytes. However, many of these show abnormal morphology after stage II and are not competent to produce functional male gametes (21). These abnormal gametocytes coexist with morphologically and functionally normal (mostly female) gametocytes, and together with them provide a total gametocytemia comparable to that of W2. In the KO parasites, the majority of sexually committed parasites arrest at early stages, leading to a dramatic reduction in the number of mature gametocytes. These differences in phenotypes could be due to a dose effect of Pfmdv-1 protein on gametocyte development. Such a dose effect could explain why reduced expression of *pfmdv-1* in Dd2 leads to some morphologically abnormal and dysfunctional gametocytes and why total disruption of the gene causes more severe effects on parasite development.

Changes in regulatory regions controlling expression may be responsible for the down-regulation of *pfmdv-1* in Dd2. To date, no nucleotide changes have been found between W2 and Dd2 in the *pfmdv-1* ORF or in its immediate noncoding flanking regions. However, efforts to sequence deep into the flanking regions have encountered difficulties because of their extremely high A+T content, including four strings of poly(A) repeats that are prone to polymerase errors.

The localization of Pfmdv-1 to PVM and CLSs and the formation of MMS after Pfmdv-1 KO show that Pfmdv-1 plays a critical role in maintaining a functional membrane network. The protein appears to be transported to the parasite surface through the secretory OB. Disruption of the *pfmdv-1* gene disturbs various gametocyte membrane structures, particularly the cleft-like extensions from PVM, leading to the formation of MMS. It is possible that resulting abnormal membrane function affects nutrient or food acquisition for the rapidly developing parasite.

We thank Drs. A. Waters and K. Williamson for discussions and advice; Dr. N. Kumar for anti-Pfg27 and -HSP70 antibodies; Dr. J. Lu for recombinant Pfmdv-1 protein; M. O'Rourke and J. Dunn-Julius for assistance in parasite culture; A. Laughinghouse and K. Lee for technical assistance; and National Institute of Allergy and Infectious Diseases intramural editor B. R. Marshall for editorial assistance. We also acknowledge support from the National Institute of Allergy and Infectious Diseases Microarray and Confocal Microscopy Facilities. This work was supported by the Intramural Research Program of the National Institutes of Health, National Institute of Allergy and Infectious Diseases.

1. Sinden, R. E. & Hartley, R. H. (1985) *J. Protozool.* **32,** 742–744.
2. Walliker, D., Quakyi, I. A., Wellems, T. E., McCutchan, T. F., Szarfman, A., London, W. T., Corcoran, L. M., Burkot, T. R. & Carter, R. (1987) *Science* **236,** 1661–1666.
3. Kaushal, D. C., Carter, R., Miller, L. H. & Krishna, G. (1980) *Nature* **286,** 490–492.
4. Smalley, M. E. & Brown, J. (1981) *Trans. R. Soc. Trop. Med. Hyg.* **75,** 316–317.
5. Brockelman, C. R. (1982) *J. Protozool.* **29,** 454–458.
6. Inselburg, J. (1983) *J. Parasitol.* **69,** 592–597.
7. Ono, T. & Nakabayashi, T. (1990) *Int. J. Parasitol.* **20,** 615–618.
8. Trager, W. & Gill, G. S. (1989) *J. Protozool.* **36,** 451–454.
9. Alano, P. & Carter, R. (1990) *Annu. Rev. Microbiol.* **44,** 429–449.
10. Ono, T., Ohnishi, Y., Nagamune, K. & Kano, M. (1993) *Exp. Parasitol.* **77,** 74–78.
11. Mann, V. H., Law, M. H., Watters, D. & Saul, A. (1996) *Int. J. Parasitol.* **26,** 117–121.
12. Robert, V., Molez, J. F. & Trape, J. F. (1996) *Am. J. Trop. Med. Hyg.* **55,** 350–351.
13. Sinden, R. E. (1998) in *Malaria: Parasite Biology, Pathology, and Protection*, ed. Sherman, I. W. (Am. Soc. Microbiol., Washington, DC), pp. 25–48.
14. Williams, J. L. (1999) *Am. J. Trop. Med. Hyg.* **60,** 7–13.
15. Dyer, M. & Day, K. (2000) *Mol. Biochem. Parasitol.* **110,** 437–448.
16. Kongkasuriyachai, D. & Kumar, N. (2002) *Int. J. Parasitol.* **32,** 1559–1566.
17. Bruce, M. C., Alano, P., Duthie, S. & Carter, R. (1990) *Parasitology* **100,** 191–200.
18. Silvestrini, F., Alano, P. & Williams, J. L. (2000) *Parasitology* **121,** 465–471.
19. Smith, T. G., Lourenco, P., Carter, R., Walliker, D. & Ranford-Cartwright, L. C. (2000) *Parasitology* **121,** 127–133.
20. Vaidya, A. B., Muratova, O., Guinet, F., Keister, D., Wellems, T. E. & Kaslow, D. C. (1995) *Mol. Biochem. Parasitol.* **69,** 65–71.
21. Guinet, F., Dvorak, J. A., Fujioka, H., Keister, D. B., Muratova, O., Kaslow, D. C., Aikawa, M., Vaidya, A. B. & Wellems, T. E. (1996) *J. Cell Biol.* **135,** 269–278.
22. Oduola, A. M., Milhous, W. K., Weatherly, N. F., Bowdre, J. H. & Desjardins, R. E. (1988) *Exp. Parasitol.* **67,** 354–360.
23. Wellems, T., Oduola, A. M. J., Fenton, B., Desjardins, R., Panton, L. J. & do Rosario, V. E. (1988) *Rev. Bras. Genet.* **11,** 813–825.
24. Wellems, T. E., Panton, L. J., Gluzman, I. Y., do Rosario, V. E., Gwadz, R. W., Walker-Jonah, A. & Krogstad, D. J. (1990) *Nature* **345,** 253–255.
25. Guinet, F. & Wellems, T. E. (1997) *Mol. Biochem. Parasitol.* **90,** 343–346.
26. Trager, W. & Jensen, J. B. (1976) *Science* **193,** 673–675.
27. Sen, S. & Churchill, G. A. (2001) *Genetics* **159,** 371–387.
28. Su, X., Ferdig, M. T., Huang, Y., Huynh, C. Q., Liu, A., You, J., Wootton, J. C. & Wellems, T. E. (1999) *Science* **286,** 1351–1353.
29. Mu, J., Duan, J., Makova, K., Joy, D. A., Huynh, C. Q., Branch, O. H., Li, W.-h. & Su, X.-z. (2002) *Nature* **418,** 323–326.
30. Bozdech, Z., Llinás, M., Pulliam, B. L., Wong, E. D., Zhu, J. & DeRisi, J. L. (2003) *PLoS Biol.* **1,** e5, 10.1371/journal.pbio.0000005.
31. Duraisingh, M. T., Triglia, T. & Cowman, A. F. (2002) *Int. J. Parasitol.* **32,** 81–89.
32. Deitsch, K., Driskill, C. & Wellems, T. (2001) *Nucleic Acids Res.* **29,** 850–853.
33. Carter, R., Ranford-Cartwright, L. & Alano, P. (1993) *Methods Mol. Biol.* **21,** 67–88.
34. Florens, L., Washburn, M. P., Raine, J. D., Anthony, R. M., Grainger, M., Haynes, J. D., Moch, J. K., Muster, N., Sacci, J. B., Tabb, D. L., *et al.* (2002) *Nature* **419,** 520–526.
35. Lasonder, E., Ishihama, Y., Andersen, J. S., Vermunt, A. M., Pain, A., Sauerwein, R. W., Eling, W. M., Hall, N., Waters, A. P., Stunnenberg, H. G., *et al.* (2002) *Nature* **419,** 537–542.
36. Silvestrini, F., Bozdech, Z., Lanfrancotti, A., Di Giulio, E., Bultrini, E., Picci, L., Derisi, J. L., Pizzi, E. & Alano, P. (2005) *Mol. Biochem. Parasitol.* **143,** 100–110.
37. Vaidya, A. B., Morrisey, J., Plowe, C. V., Kaslow, D. C. & Wellems, T. E. (1993) *Mol. Cell. Biol.* **13,** 7349–7357.